Nuclear magnetic resonance in molten In-InI_3 mixtures

K. Ichikawa
Department of Chemistry, Hokkaido University, Sapporo 060, Japan

W. W. Warren, Jr.
Bell Laboratories, Murray Hill, New Jersey 07974

(Received 29 January 1979)

Nuclear-magnetic-resonance data are reported for molten $In_{1-x}I_x$ mixtures with compositions in the range $0 \leq x \leq 0.75$ and at temperatures ranging from the liquidus up to 600–1200 °C, depending on composition. Mixtures in the range $0 < x < 0.50$ form two immiscible phases which are clearly indicated by distinct ^{115}In resonance lines and which remain separated to temperatures in excess of 1000 °C. Chemical shifts in single-phase mixtures ($x \geq 0.50$) exhibit a systematic increase with I content. The ^{115}In spin-lattice relaxation rates ($1/T_1$) and inverse free-induction decay lifetimes ($1/T_2^*$) are attributed to at least two processes: quadrupolar relaxation via ionic and molecular motion and a strong scalar magnetic coupling to paramagnetic centers. The composition dependence of the quadrupolar process, also observed for ^{127}I, shows that the degree of dissociation increases with decreasing I content. The behavior of the scalar magnetic process in phase-separated mixtures ($x < 0.50$) supports the *F*-center model for dissolved In in InI. It is proposed that the scalar relaxation in single-phase mixtures ($x \geq 0.50$) results from short-lived fluctuations to the paramagnetic In^{2+} state by single-electron hopping. The theory of relaxation by magnetic scalar coupling is generalized to allow for the large hyperfine couplings present. The generalized theory is in agreement with the experimental results and permits estimates of the frequency of electron hopping and the lifetime of the In^{2+} state.

I. INTRODUCTION

Although the study of liquid mixtures of metals with their molten salts has a long history,[1] there have been few investigations of these interesting systems employing microscopic experimental probes. Rather, emphasis has been placed mainly on the determination of thermodynamic properties (phase diagram, vapor pressure, density, etc.) and macroscopic transport properties (electrical conductivity, viscosity, etc.). In particular, it is only recently that the techniques of electron spin resonance (ESR) and nuclear magnetic resonance (NMR) have been applied to this class of system.[2,3] Such experiments are of considerable value in revealing microscopic details of a number of interesting phenomena occurring in molten metal-salt mixtures. Examples of such phenomena or areas of interest are the metal-nonmetal transition, nonmetallic electron dynamics, microscopic inhomogeneity and concentration fluctuations, and the molecular or ionic arrangements and their dynamic properties.

This paper describes an NMR investigation of liquid In-InI_3 mixtures. This system was chosen primarily because of the presence of two "sub-halides" InI and InI_2 whose existence as well-defined crystalline phases is clearly evident from the phase diagram (Fig. 1)[4] and far-infrared spectroscopy.[5] In this respect

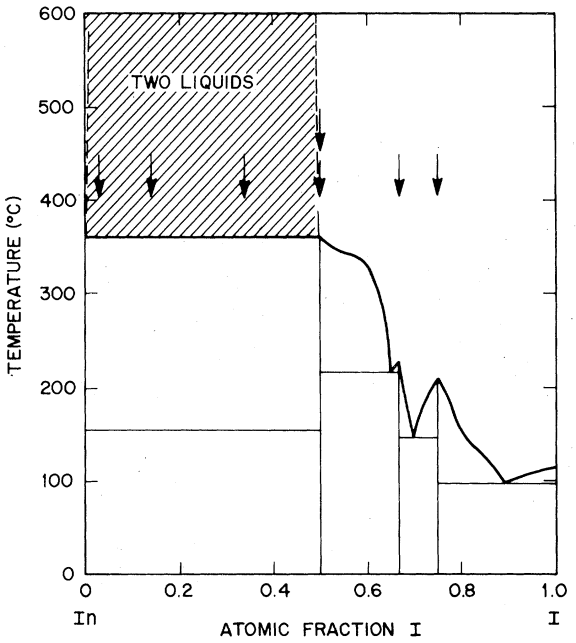

FIG. 1. Phase diagram of the In-I system (Ref. 4). The shaded region indicates the wide region of liquid immiscibility between In and InI. The congruently melting solid compounds are InI, InI_2, and InI_3. Arrows indicate compositions of samples studied in the present work.

the In-InI_3 system is quite different from systems such as the alkali metal-halide mixtures or Bi-BiI_3, for which no intermediate phases persist up to the temperature of the liquidus.[1] In fact, the restricted concentration range In-InI may be viewed as an analogue of the alkali metal-halide mixtures. Thus within the full composition range In-InI_3 there should exist both a metal-nonmetal transition and a region containing at least two distinct valence states, In^+ and In^{3+}. Additional features of this system which make it attractive from the experimental point of view are the presence of two abundant and strongly magnetic nuclei, ^{115}In and ^{127}I, as well as its relative chemical stability in quartz containers over a wide range of temperatures in the liquid state.

Previous work on liquid In-InI_3 is not extensive but does include, in addition to the phase diagram determinations, electrochemical measurement of the chemical potential[6] and the dc electrical conductivity.[7] In addition various investigations of molten InI_3 have been carried out, namely, measurements of the density,[8,9] viscosity[10] and dc conductivity[8] as well as liquid-structure determinations using x-ray diffraction[11] and Raman and infrared spectroscopy.[12] These data indicate that the structure of InI_3 is predominantly molecular, based on the In_2I_6 dimer, although the value of the dc conductivity [$\kappa \simeq 0.1\ (\Omega\ \text{cm})^{-1}$] is high enough to suggest some dissociation to form mobile ions.[7,8] The considerably higher conductivity of liquid InI[7] [$\kappa \gtrsim 1\ (\Omega\ \text{cm})^{-1}$] is comparable with those of the molten alkali iodides suggesting nearly complete dissociation

$$InI \rightarrow In^+ + I^- \ . \tag{1}$$

A qualitatively similar trend has been observed for GaI-GaI_3 mixtures although the degree of dissociation of GaI_3 just above the melting point is considerably lower than that of InI_3.[13]

In this investigation we have studied three mixtures $In_{1-x}I_x$ whose compositions lie in the region of the liquid-liquid phase separation ($x = 0.03$, 0.14, and 0.34) and four single-phase samples whose compositions are nominally InI (two samples), InI_2 and InI_3 (see Fig. 1). The data include ^{115}In Knight and chemical shifts, spin-spin and spin-lattice relaxation times (T_2 and T_1, respectively) and where possible, similar relaxation times for ^{127}I. The ^{127}I data are necessarily less extensive because of prohibitively large NMR linewidths for some compositions.

The organization of this paper is as follows: in Sec. II we present essential details of the experimental technique and apparatus; Sec. III contains the experimental results; these results are discussed and a physical interpretation is developed in Sec. IV; finally, we summarize in Sec. V the main results and conclusions of the work.

II. EXPERIMENTAL DETAILS

The samples used in these experiments were prepared from weighed amounts of elemental In (99.9999%) and InI_3 (Alfa-Ventron "Ultra-pure") which were sealed under vacuum in quartz sample cells. All handling of the materials prior to sealing was carried out in a dry box containing a purified argon atmosphere. The mixtures were formed in situ in the high-temperature NMR apparatus and in some cases the molten mixtures were shaken by hand to improve homogeneity. After melting, the sample material typically occupied about half the volume of the cells (5 mm i.d. × 10 mm length). The sample compositions quoted correspond to the weighed amounts of starting material.

The high-temperature NMR apparatus was based on a Pt radio-frequency sample coil cast into a ceramic form and contained within a noninductive Pt heater wound on an Al_2O_3 ceramic tube. The rf coil was designed to fit closely around the quartz sample cells. The entire assembly of rf coil, sample, and heater was surrounded by thermal insulation and was contained within a cylindrical water-cooled brass jacket. The latter just fit into the 76-mm magnet gap.

Sample temperatures were measured by a Pt vs Pt-10% Rh thermocouple. The junction was located in a re-entrant well protruding into the sample cell. As a check on the absolute accuracy of our temperature determinations, the observed melting temperature of one InI sample was compared with the phase diagram[4] and found to agree within 3 °C. The thermocouple output was also employed in a simple temperature regulation system which maintained constant sample temperatures within ±1 °C during the course of the measurements.

The ^{115}In and ^{127}I NMR signals were observed with a coherent transient NMR spectrometer. The majority of the data were taken at a frequency of 16.0 MHz with more limited measurements being carried out at 9.5 and 5.5 MHz. A dual-channel boxcar integrator[14] was used for signal-to-noise enhancement and as an integrator to obtain field-sweep Fourier transform displays.[15] The Knight- and chemical-shift measurements were referred to a reference field for ^{115}In NMR in an aqueous solution of $In_2(SO_4)_3$. The stability and reproducibility of the magnetic field were monitored using an auxiliary ^2H resonance in D_2O.

Spin-spin relaxation times T_2 were determined from the free-induction decay lifetimes T_2^*. Since these decay rates were much faster than might be expected from inhomogeneous broadening and since no spin echoes could be observed, we have assumed $T_2 = T_2^*$. Spin-lattice relaxation times T_1 were measured with the standard two pulse $\pi - \frac{1}{2}\pi$ sequence. In certain ranges of temperature and composition the relaxation times were so short that measurements became impossible. Measurement of T_1 was limited to

temperature ranges such that T_1 was longer than about 10 μsec and T_2^* was more than 3 μsec. The shortest T_2^* value we were able to measure was about 1.5 μsec.

III. EXPERIMENTAL RESULTS

A. Resonance shifts

The composition dependence of the resonance shift is illustrated qualitatively in Fig. 2 in which typical absorption spectra are reproduced for selected compositions. The metal-rich mixtures ($x < 0.50$) consistently yielded two resonance lines near the magnetic field values corresponding to In and InI, respectively. Our attempts to achieve homogeneous single-phase liquids in this composition range by raising the temperature above the consolute point were unsuccessful. The widely separated resonances persisted to temperatures in excess of 1000 °C even when the samples were vigorously agitated. This indicates that the consolute temperature is very high in this system, certainly well above 1000 °C, since we observed only the slightest tendency for the two lines to converge on a common position over the range of temperatures investigated. The second main feature of the data shown in Fig. 2 is the shift to higher values of resonance magnetic field observed with increasing I concentration for the single-phase salt-rich mixtures ($x \geq 0.50$).

Although both Knight shifts (K) and chemical shifts (δ) must be considered for a metal-salt solution we have chosen arbitrarily to define shifts as if they were Knight shifts in order to obtain a common plot. Such a choice is necessary because of an unfortunate

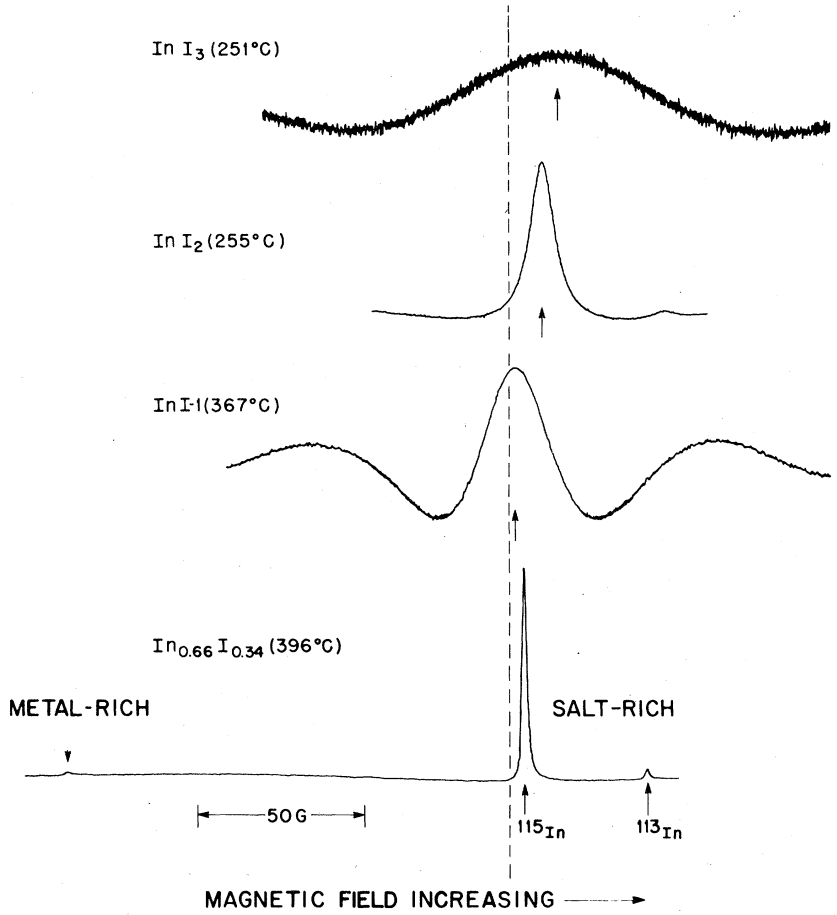

FIG. 2. Representative ^{115}In NMR absorption spectra in liquid $In_{1-x}I_x$ mixtures. The displays shown were obtained by Fourier transformation of free-induction decay transients using the method of Ref. 15. Distortion of the wider lines, especially for InI_3 and InI-1, results from loss of the initial portion of the free-induction decay due to the finite receiver recovery time (~5 μsec). For $x = 0.34$ and InI_2 the weak ^{113}In resonance is also visible. In the two-phase alloy $x = 0.34$, the relatively low intensity of the signal from the metal-rich phase results from the small radio-frequency skin depth. Vertical broken line indicates resonance position for aqueous $In_2(SO_4)_3$ reference solution.

difference in the conventional definitions of K and δ. If we denote by H_0 and H_{ref} the respective resonant field values of the sample and of the reference material at constant frequency, then the Knight shift is defined according to $K \equiv (H_{ref} - H_0)/H_0$. The chemical shift, on the other hand, is conventionally defined by $\delta \equiv (H_0 - H_{ref})/H_{ref}$. Thus, since $|\delta| << 1$, we have $\delta = -K(H_0/H_{ref}) \simeq -K$.

Our shift data, represented as "Knight shifts," are plotted versus temperature in Fig. 3. Data for three samples in the two-phase region ($x < 0.50$) fall on two common branches. Shift values on the metal-rich branch exhibit essentially the same temperature dependence as that observed for pure liquid In,[16] while the magnitudes of the shifts in the mixtures were larger than for pure In by an average of 0.012%. Whether or not this difference is due to a systematic difference in the absolute shift calibrations, it is evident that the metal-rich shifts in the mixtures are very close to those of pure In.

Shift values in the salt-rich phase of the two-phase mixtures agree within experimental error with the shifts observed for single-phase mixtures having compositions close to InI. As the temperature was increased, the salt-rich line in the two-phase mixtures shifted toward positive K values, that is, toward the shift value of the metal-rich phase. This is a small effect, however, compared with the large difference in shifts of the two phases. For example, the splitting between the metal- and salt-rich resonances decreases by only about 10% between 370 and 1000 °C and roughly half this change is due to the negative temperature coefficient of the metal-rich shift, also observed for pure In. Thus any reduction of the splitting due to changes in concentration as the consolute temperature is approached must be very small, no more than a few percent.

The resonance shifts in the single-phase mixtures were not measured over wide temperature ranges because of greatly increased linewidths at higher temperatures. Within the ranges investigated, no temperature dependences could be resolved for these mixtures. However, a dependence on concentration was found and we observed a clear progression with increasing I concentration toward more negative K values, i.e., toward larger, positive chemical shift. Taking averages over all measurements for each composition we find the following chemical-shift values:

$$InI \quad \delta = 2.2 \pm 1.0 \times 10^{-4} ,$$

$$InI_2 \quad \delta = 5.6 \pm 0.2 \times 10^{-4} ,$$

$$InI_3 \quad \delta = 7.8 \pm 1.0 \times 10^{-4} .$$

B. Relaxation rates

Spin-lattice relaxation rates ($1/T_1$) and inverse free-induction decay lifetimes ($1/T_2^*$) are shown in Figs. 4–7 for $x = 0.34$ (salt-rich phase) and for single-phase mixtures InI, InI_2, and InI_3, respectively. The data have been plotted in the form ln(rate) vs $1/T$ as a means of identifying those relaxation

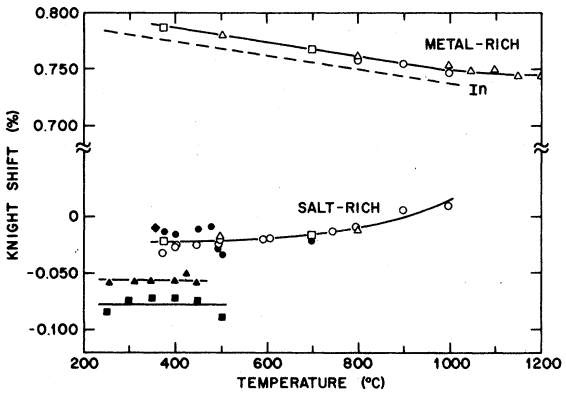

FIG. 3. ^{115}In resonance shifts for liquid $In_{1-x}I_x$ mixtures plotted as Knight shifts vs temperature for various compositions. Open points denote data in phase-separated liquid mixtures with $x < 0.50$: triangles, $x = 0.035$; squares, $x = 0.14$; circles, 0.34; closed points denote shifts in single-phase mixtures with $x \geq 0.50$: circles, InI-1; diamonds, InI-2; triangles, InI_2; squares, InI_3. Broken line represents data for pure liquid In (Ref. 16). Note discontinuity in vertical scale.

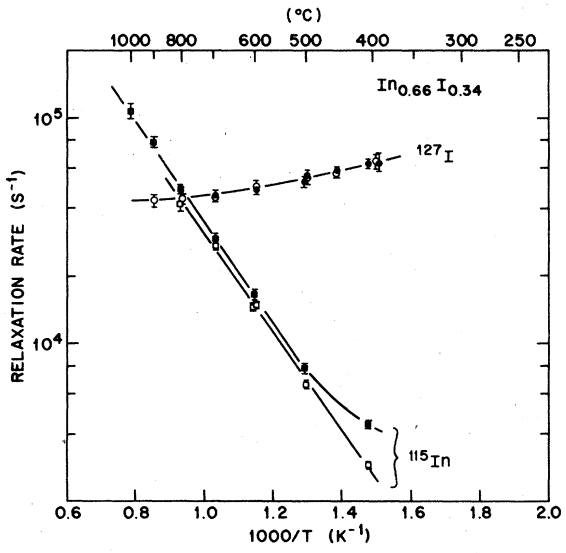

FIG. 4. Logarithm of the relaxation rates vs inverse temperature for ^{115}In (squares) and ^{127}I (circles) in liquid mixture of composition $In_{0.66}I_{0.34}$. Open points are spin-lattice relaxation rates ($1/T_1$) and closed points are free-induction decay lifetimes ($1/T_2^*$). Data are for salt-rich phase of this two-phase mixture.

processes having exponentially activated temperature dependences.

The relaxation data shown in Figs. 4–7 are quite complex and strikingly different behavior appears for different compositions. Although it is difficult to summarize the qualitative features, some systematics of the ^{115}In rates are evident:

(i) ^{115}In rates in every sample increase with temperature at sufficiently high temperature, and the dependence can be represented as exponentially activated.

(ii) In the two samples having the highest I content, the ^{115}In rates initially decrease with temperature at the lowest temperatures.

(iii) Values of $1/T_2{}^*$ for ^{115}In generally exceed $1/T_1$, most notably for InI and InI_2. These rates become equal at the lowest temperatures for InI_2 and are nearly equal for the salt-rich phase of $x = 0.34$.

After initial formation of the mixtures, all relaxation rates were found to be reversible with respect to heating and cooling and in those cases checked, the data were reproducible after cooling to room temperature and remelting in subsequent runs.

The frequency dependences of the ^{115}In relaxation rates were investigated and differing behavior was observed for different compositions. For InI, $1/T_1$ decreases with increasing frequency while $1/T_2{}^*$ is nearly constant (increasing slightly for InI-1). For InI_2,

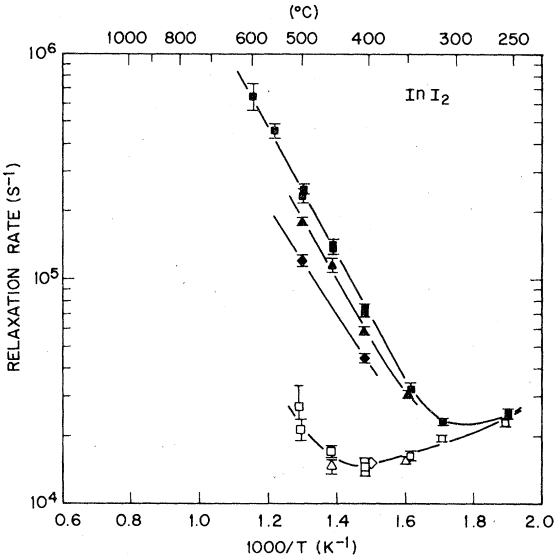

FIG. 6. Logarithm of the relaxation rates vs inverse temperature for ^{115}In in liquid mixture of nominal composition InI_2. Open points, spin-lattice relaxation rates ($1/T_1$); closed points, free-induction decay lifetimes ($1/T_2{}^*$); squares, 16.0 MHz; triangles, 9.5 MHz; diamonds, 5.5 MHz.

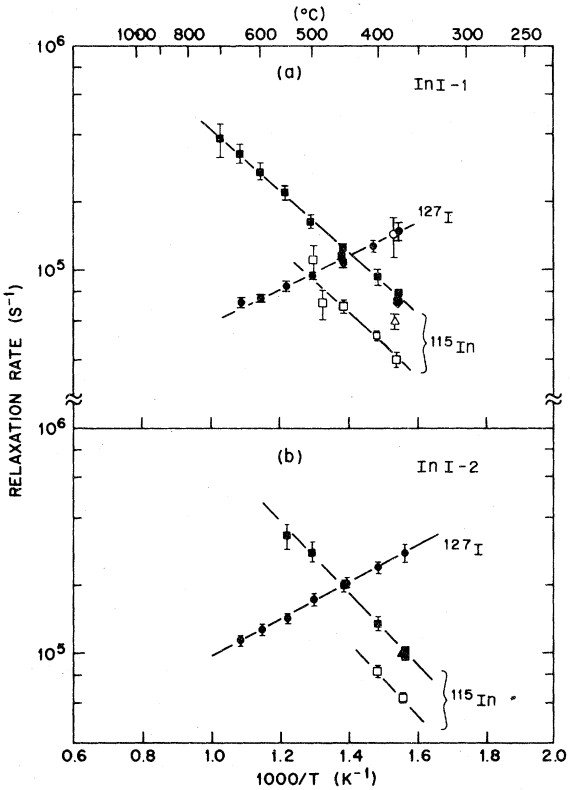

FIG. 5. Logarithm of the relaxation rates vs inverse temperature for ^{115}In and ^{127}I in two liquid samples of nominal composition InI. Open points, spin-lattice relaxation rates ($1/T_2$); closed points, free-induction decay lifetimes ($1/T_2{}^*$); squares, ^{115}In at 16.0 MHz; triangles, ^{115}In at 9.5 MHz; diamonds, ^{115}In at 5.5 MHz; circles, ^{127}I at 16.0 MHz.

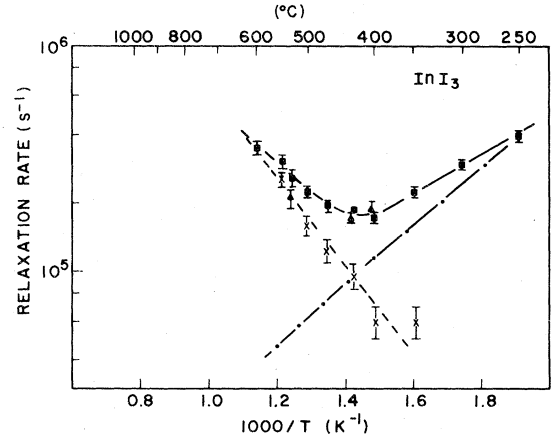

FIG. 7. Logarithm of the free-induction decay lifetime ($1/T_2{}^*$) vs inverse temperature for ^{115}In in liquid InI_3 at 16.0 MHz (squares) and 9.5 MHz (triangles). Solid points denote expected temperature dependence of quadrupolar relaxation [Eqs. (6) and (7)] normalized to data at 250 °C. Crosses denote difference between measured rates and expected quadrupolar rates.

on the other hand, $1/T_2{}^*$ increases sharply with frequency in the high-temperature range but is independent of frequency at lower temperatures where the negative temperature dependence is observed. The spin-lattice relaxation rates $1/T_1$ are likewise independent of frequency at low temperatures; at high temperatures, the frequency dependence could not be resolved due to poor signal-to-noise ratios.

The ^{127}I resonance could be observed only in the samples having lower I content and the relaxation rates increase with increasing x. It seems quite likely that the ^{127}I resonance is unobservably broad for InI_2 and InI_3. The ^{127}I relaxation rates invariably decrease with temperature, even in temperature and composition ranges where the ^{115}In rates increase strongly. Whenever both rates could be measured for ^{127}I, we observed $1/T_2{}^* = 1/T_1$.

IV. ANALYSIS AND INTERPRETATION

The existence of a wide region of liquid-liquid phase separation with a very high consolute temperature leads naturally to division of the discussion of the properties of liquid In-InI_3 mixtures. We shall therefore consider first the region $x \geq 0.50$ containing single-phase, nonmetallic molten salts and then turn our attention to the phase-separated liquids with $x < 0.50$. This situation, incidentally, contrasts sharply with that of Bi-BiI_3 investigated previously.[3] That system contains no apparent intermediate subhalides in the liquid state and the consolute temperature is relatively low. A further important difference is that large ^{209}Bi Knight-shift values were observed in mixtures approaching the concentration of BiI_3 whereas, we have observed no Knight shifts of "metallic" magnitude for $x \gtrsim 0.50$. This suggests that the intermediate compound InI with valence state In^+ is crucially relevant to the properties of this system and we shall take this into account when developing an interpretation of our NMR data.

A. Single-phase mixtures ($x \geq 0.50$)

1. Chemical shifts

The first systematic investigation of chemical shifts in molten salts was carried out by Hafner and Nachtrieb.[17] They ascribed a systematic decrease of the chemical shift δ to increasing covalency in a series of molten Tl salts. This behavior was explained in terms of the Ramsey theory[18] of chemical shifts as a change in the so-called "paramagnetic" contribution which can be expressed in the approximate form

$$\delta_P = -\frac{16}{3}\mu_B^2 \left\langle \frac{1}{r^3} \right\rangle \left(\frac{B}{\Delta E} \right) , \qquad (2)$$

in which μ_B is the Bohr magneton, r is the electron radial coordinate, $\langle\ \rangle$ represents an average over the covalent state wavefunction, B is a measure of the covalency or overlap, and ΔE is an average energy of excitation from the ionic ground state to the low-lying excited states. Thus increasing covalency (B) leads to a reduction in chemical shift due to the negative sign on the right-hand side of Eq. (2).

The trend of chemical shifts in In-InI_3 single-phase mixtures is contrary to expectations based on the work of Hafner and Nachtrieb in Tl salts.[17] In the first place we have observed that ^{115}In in molten InI_3 has a *positive* chemical shift relative to In^{3+} in aqueous solution. However, the tetrahedral coordination of In in crystalline InI_3 (Ref. 19) and the evidence for molecular structure in molten InI_3 (Refs. 11 and 12) suggest considerable covalency. Hence, by Eq. (2), a negative shift relative to the free-ion would be expected. Second, conductivity data in In-InI_3,[7] and the related system Ga-GaI_3,[13] indicate increasing covalency (i.e., lower ionic conductivity) with increasing I content. But this is opposite to the trend we have observed whereby the chemical shift increases with increasing x from InI to InI_3.

The difference between our results and the observations in Tl salts points out the danger of overreliance on the simplified expression given in Eq. (2) and of neglect of the effect of chemical environment on the factors $\langle 1/r^3 \rangle$ and ΔE. The effect on $\langle 1/r^3 \rangle$ of changing covalency has been discussed, for example, by Lütgemeier[20] who studied chemical shift trends in various series of crystalline III-V compounds. It was found that the chemical shifts increase with covalency in a series such as ^{115}In in In-InAs-InSb. Lütgemeier argued that the electron charge density should contract with increasing ionicity, thus increasing $\langle 1/r^3 \rangle$ and hence decreasing δ. The situation is more complicated for In-InI_3 mixtures, since the relevant ionic state changes from In^+ to In^{3+} as the I content is varied. Thus it is likely that changes occur in all parameters in Eq. (2) as well as in the diamagnetic contribution δ_d as the composition is varied. Lacking a more sophisticated theory we feel that an attempt to extract a quantitative measure of covalency from the present data would be unjustified and the results unreliable.

2. Relaxation rates

The relaxation rate measurements in single-phase mixtures suggest the presence of at least two types of relaxation process in these liquids. The first process, observed for ^{127}I when $x \simeq 0.50$ and for ^{115}In at low temperature in InI_2 and InI_3, is characterized by $1/T_1 = 1/T_2$, the absence of frequency dependence, and by rates which decrease with increasing temperature. These features are characteristic of electric quad-

rupolar relaxation driven by molecular and ionic motions.[21] Of particular importance are rotational motions of molecular units or complex ions. Relaxation of this type has been observed previously in molten sodium nitrate,[22] certain liquid tellurium alloys,[23–25] and numerous molecular liquids.[26]

The second relaxation process exhibits several very unusual features which distinguish these mixtures from other classes of liquid. Most notable among these are the progressively stronger relaxation rates observed for ^{115}In in all compositions at sufficiently high temperature. In general, $1/T_1 \neq 1/T_2$ in this range and the rates depend on frequency. The process is specific to ^{115}In since none of these features is observed for ^{127}I, even in situations where this mechanism dominates the ^{115}In relaxation. We believe this process to be related to the presence in these mixtures of more than one valence state and to the possibility of short-lived fluctuations to a paramagnetic state In^{2+}. We shall refer to this mechanism as relaxation by paramagnetic valence fluctuations. Interpretation of the relaxation rate data in terms of these two mechanisms will be developed in more detail below:

a. Electric quadrupolar relaxation via ionic and molecular motion. In general any nucleus with spin greater than $\frac{1}{2}$ experiences an electrostatic coupling with the gradient of the local electric field. Because the interaction vanishes when the nuclear environment has cubic symmetry, rapid rotational, and diffusive motions in liquids normally lead to a vanishing time-averaged quadrupolar interaction. Thus there are no shifts or splittings due to the quadrupole interaction except in special classes of liquid such as liquid crystals. On the other hand, the *instantaneous* electric field gradient is noncubic, in general, and the resulting time-dependent quadrupole interaction can be very effective in producing nuclear spin relaxation.

The quadrupolar relaxation rate can be expressed conveniently in terms of spectral density functions for the time-dependent electric field gradient (efg). When, as is usually true in liquids, the efg fluctuates at a rate fast compared with the nuclear Larmor frequency ω_0, the general expression for the relaxation rates can be written[21]

$$\left(\frac{1}{T_1}\right)_Q = \left(\frac{1}{T_2}\right)_Q = \tfrac{3}{4} f(I) \left(\frac{eQ}{\hbar}\right)^2 J(0) \quad , \tag{3}$$

where

$$f(I) = (2I+3)/I^2(2I-1) \quad .$$

The spectral functions

$$J(0) = J_1(\omega_0) = J_2(2\omega_0)$$

are obtained by Fourier transformation of the time correlation functions for appropriate components V_{ij} of the efg

$$J_m(m\omega_0) = \int_{-\infty}^{\infty} e^{-im\omega_0 t} \langle V^m(t) V^{-m}(0) \rangle_{av} dt \quad , \tag{4}$$

where

$$V^{\pm 1} = (1/\sqrt{6})[V_{xz}(t) \pm iV_{yz}(t)] \quad , \tag{5a}$$

$$V^{\pm 2} = (1/2\sqrt{6})[V_{xx}(t) - V_{yy}(t) \pm 2iV_{xy}(t)] \quad . \tag{5b}$$

In the special case of a rapidly rotating molecule or complex ion, Eq. (4) takes the form[21]

$$\left(\frac{1}{T_1}\right)_Q = \left(\frac{1}{T_2}\right)_Q = \tfrac{3}{40} f(I) \left(1 + \frac{\sigma^2}{3}\right) \left(\frac{e^2qQ}{\hbar}\right)^2 \tau_c \quad , \tag{6}$$

where q is the efg along the molecular principal axis, σ is the asymmetry parameter of the efg, and τ_c is a correlation time characterizing the rate of fluctuation of the efg projected on the laboratory coordinate system.

X-ray diffraction and vibrational spectroscopy studies have indicated the presence of well-defined molecular structures in liquid InI_3.[11,12] Although it was not possible to establish from the x-ray measurements whether the monomer or the In_2I_6 dimer is predominant,[11] the more recent Raman and infrared spectra have been successfully indexed using the dimer model.[12] The dimer also exists in crystalline InI_3 so that we can employ values of e^2qQ and σ obtained by nuclear quadrupolar resonance (NQR) in the solid to estimate the expected ^{115}In quadrupolar rate in molecular-liquid InI_3 predicted by Eq. (6). The correlation time can be estimated from the measured viscosity (η) by assuming a rotating spherical molecule of radius r_0

$$\tau_c = \frac{4\pi r_0^3}{3k} \frac{\eta}{T} \quad . \tag{7}$$

We take $r_0 \sim 3.6 \times 10^{-8}$ cm,[11] $T = 553$ K, $\eta = 3.73$ cP,[10] and from NQR at 300 K,[27] $(e^2qQ/h) = 321$ MHz with $\sigma = 0.69$. When substituted into Eq. (6) these parameters yield

$$\left(\frac{1}{T_1}\right)_Q \simeq 2.5 \times 10^6 \text{ sec}^{-1} \quad .$$

An estimate of r_0 using the molar volume of InI_3,[8,9] yields $r_0 \simeq 3.8 \times 10^{-8}$ cm and a comparable value of $(1/T_1)_Q$. In contrast the experimental value is roughly an order of magnitude smaller

$$\left(\frac{1}{T_1}\right)_Q = 3.3 \pm 0.2 \times 10^5 \text{ sec}^{-1} \quad .$$

The higher relaxation rate predicted by theory is not surprising, however, given the approximations of the calculation, particularly the use of Eq. (7), and the assumption of a rotating sphere. Furthermore, it is quite plausible that the actual correlation time is shorter than given by Eq. (7) as a result of partial dissociation which effectively reduces r_0. The relatively high electrical conductivity [$\kappa \simeq 0.1$ $(\Omega\ \text{cm})^{-1}$] of molten InI_3 shows that the liquid is not fully molecular.

The temperature dependence of the quadrupolar relaxation rate predicted by Eq. (6) is $(1/T_1)_Q \propto \tau_c \propto \eta/T$. (We neglect changes in the molecular efg and asymmetry parameter since these are likely to be small compared with the variation of τ_c.) The temperature dependence of η/T is compared with the data in Fig. 7, where it can be seen to decrease more rapidly than the observed relaxation rate. However, this is easily explained as the effect of the additional relaxation process which increases with temperature. As may be seen, the data can be represented as the sum of a quadrupolar rate proportional to η/T and an exponentially increasing rate. (The origin of the latter will be considered in detail shortly.) Thus both the magnitude and temperature dependence of the ^{115}In relaxation rate in InI_3 at low temperatures are consistent with the quadrupolar mechanism described by Eq. (6).

We have so far considered only the ^{115}In relaxation in liquid InI_3. We can estimate the expected ^{127}I rate by scaling the observed ^{115}In rates according to Eq. (6), using values of the e^2qQ and σ measured for ^{127}I in crystalline InI_3. This procedure is complicated somewhat by the presence in the crystal of two types of ^{127}I site having rather different efg values. These are the bridging and outer I sites in the In_2I_6 dimer. The NQR data[28] yield the values

$$\left(1+\frac{\sigma^2}{3}\right)\left(\frac{e^2qQ}{h}\right)^2 = \begin{cases} 0.608\times10^6\ \text{MHz}^2\ \text{(bridging)} \\ 1.334\times10^6\ \text{MHz}^2\ \text{(outer)} \end{cases}$$

Assuming rapid interchange between the two types of site we average the above values, taking into account the weighting of two bridging and four outer I atoms per molecule. Thus

$$\left(1+\frac{\sigma^2}{3}\right)\left(\frac{e^2qQ}{h}\right)^2 \simeq 1.1\times10^6\ \text{MHz}^2$$

and from Eq. (6)

$$\left(\frac{1}{T_1}\right)_Q^{127} \Big/ \left(\frac{1}{T_1}\right)_Q^{115} \simeq 40\ .$$

Since we have

$$(1/T_2)^{115} = 3.3\times10^5\ \text{sec}^{-1}$$

for the ^{115}In relaxation rate at 280 °C, we might expect

$$(1/T_1)^{127} \simeq (1/T_2)^{127} \simeq 1.3\times10^7\ \text{sec}^{-1}$$

or $T_1 \sim 77$ ns for ^{127}I. This relaxation time is much shorter than the minimum ($T_2^* \sim 1$–2 μsec) that we require in order to observe a resonance and this easily explains the absence of an NMR signal for ^{127}I in InI_3.

If the molecular structure tends to dissociate when x decreases, as suggested by the conductivity data, we would expect lower values of the quadrupolar relaxation rate. This is because τ_c becomes shorter in the dissociated liquid and because the efg tends to be smaller when the bonding is more ionic. This is evidently the case for InI_2 where the low-temperature relaxation rate is roughly an order of magnitude smaller than for InI_3. The ^{127}I rate should also be smaller although a scaling argument like that described above predicts $(1/T_1)_Q^{127} \sim 1\times10^6\ \text{sec}^{-1}$ which would still render the resonance extremely difficult to observe. For InI, on the other hand, the ^{127}I signal is visible with values of T_2^* greater than about 3 μsec. The corresponding ^{115}In quadrupolar rate should therefore be

$$(1/T_1)_Q^{115} \sim 5\times10^3\ \text{sec}^{-1}\ .$$

This is nearly two orders of magnitude *smaller* than the rates observed experimentally and the experimental rates only increase with temperature over the entire range investigated. We conclude therefore that the ^{115}In quadrupolar rate in mixtures close to the composition of InI is sufficiently low as to be overwhelmed by the additional relaxation process which increases with temperature. We must now consider this second process.

b. Relaxation due to magnetic valence fluctuations. (i) Theoretical considerations: At sufficiently high temperatures, the relaxation rates in all single-phase mixtures are dominated by a process which increases rapidly with temperature, for which T_1 is not equal to T_2, and which is specific to the ^{115}In nuclei. These features are highly unusual in liquids. In all but the most viscous liquids, rapid atomic motion typically leads to a relaxation rate proportional to a correlation time characterizing the rate of fluctuation of the local environment. [A particular example of this is the quadrupolar rate described by Eq. (6).] In this situation, the so-called "extreme narrowing" limit, T_1 and T_2 are equal and independent of frequency.[29] The temperature dependences of the rates are governed by the correlation time and this normally shortens with increasing temperature leading to lower relaxation rates at high temperatures. None of these "normal" characteristics is observed for the ^{115}In relaxation in the single-phase mixtures at high temperature.

An additional difficulty is raised by the surprising strength of the high-temperature relaxation process.

The observed rates ($\sim 10^5$ sec) are several orders of magnitude larger than typically observed for various other mechanisms active in nonmetallic liquids: relaxation by dipole-dipole interactions,[29] and anisotropic chemical shift,[29] or spin-rotational interactions.[30] Moreover, there is no apparent reason why any of these mechanisms should be so much more effective for ^{115}In than for ^{127}I. Still another mechanism, relaxation of ^{115}In by scalar coupling to rapidly relaxing ^{127}I nuclei, has sufficient potential strength. But for this process, T_1 and T_2 become equal when the two species exhibit opposing temperature dependences such as those observed for ^{115}In and ^{127}I in InI-1 and InI-2.[31] Thus none of these standard relaxation mechanisms can be invoked to explain the present data.

We propose that the unusual high-temperature relaxation behavior in single-phase In-InI_3 mixtures is due to the presence of two stable ionic states In^+ and In^{3+} and to the consequent possibility of fluctuations to the paramagnetic state In^{2+} by a one-electron transfer process

$$In^+ + In^{3+} \rightarrow 2In^{2+} \quad . \tag{8}$$

Since the single 5s-electron of the In^{2+} ion produces a hyperfine field on the order of 10 MG (Ref. 32), fluctuation into the In^{2+} state leads to powerful time-dependent local fields at the nuclei. The effectiveness of these fluctuations in producing nuclear relaxation depends on the instantaneous probability P that a nucleus will be in an In^{2+} ion and on the time-dependent properties of the In^{2+} state itself.

The probability P is determined by the concentrations of various chemical species present in the mixture and by the free-energy change associated with the fluctuation. We assume that at least four possible bonding states may be present for In in the single-phase mixtures: two ionic states In^+ and In^{3+} and two covalent bonding states associated with the molecule In_2I_6 and the complex ion $(InI_4)^-$. The concentrations of these species depend on the composition of the mixture and on the equilibria of the following reactions:

$$2In + InI_3 \rightarrow 3In^+ + 3I^- \quad , \tag{9}$$

$$2In + 4InI_3 \rightarrow 3In^+ + 3(InI_4)^- \quad , \tag{10}$$

$$(InI_4)^- \rightarrow In^{3+} + 4I^- \quad , \tag{11}$$

$$InI_3 \rightarrow In^{3+} + 3I^- \quad . \tag{12}$$

It is clear that, in general, there will be equilibrium concentrations of both In^+ and In^{3+}, and that the concentration of In^{3+} can be expected to increase at higher temperatures due to the dissociation reactions (11) and (12). Stoichiometric InI_3 should not contain In^+, but this species could be generated at high temperatures by decomposition

$$InI_3 \rightarrow In^+ + I^- + I_2 \quad . \tag{13}$$

The instantaneous probability p_1 that a particular In nucleus will be a member of a pair of neighboring In^+-In^{3+} ions will be

$$p_1 \simeq z c(In^+) c(In^{3+}) \quad , \tag{14}$$

where z is the mean In-In first-neighbor coordination number and $c(In^+)$ and $c(In^{3+})$ are, respectively, the fractional concentrations of In^+ and In^{3+}. As a first approximation, if we consider only the reactions (9)–(12) and assume that InI is fully dissociated as suggested by its relatively high electrical conductivity, then $c(In^+)$ depends only on the concentration x of the mixture

$$c(In^+) \simeq \frac{4x-3}{2(x-1)} \quad . \tag{15}$$

The concentration of In^{3+}, on the other hand, depends on the dissociation reactions (11) and (12) and should exhibit an approximately exponential temperature dependence

$$c(In^{3+}) \simeq c_3(x) \exp(-\Delta H_3/RT) \quad , \tag{16}$$

where ΔH_3 is the heat of reaction for whichever equilibrium limits the concentration of In^{3+}, and the prefactor $c_3(x)$ depends only on concentration.

Now given a pair of neighboring In^+ and In^{3+} ions, the probability that this pair will be in the state In^{2+}-In^{2+} is $\exp[-(\Delta H_2 - T\Delta S_2)/RT]$, where ΔH_2 and ΔS_2 are, respectively, the enthalpy and entropy changes associated with the fluctuation. Thus, finally, the probability that a particular In nucleus will be in a state In^{2+} is,

$$P = p_0 \exp[-(\Delta H_3 + \tfrac{1}{2}\Delta H_2)/RT] \quad , \tag{17}$$

where

$$p_0 \cong z \frac{(4x-3)}{2(x-1)} c_3(x) \exp[\Delta S_2/2R] \quad . \tag{18}$$

The factor $\frac{1}{2}$ multiplying ΔH_2 and ΔS_2 in the arguments of the exponentials accounts for the fact that a single fluctuation, i.e., a single-electron transfer, produces *two* nuclei in the In^{2+} state.

In addition to their dependence on the probability P, the nuclear relaxation rates also depend on the dynamic properties of the paramagnetic state In^{2+} since these determine the time dependence of the local magnetic hyperfine field. The physical situation is similar to the more familiar example of relaxation in a liquid by scalar interaction with a paramagnetic impurity, e.g., proton relaxation in H_2O by dissolved Mn^{++}.[33] The general theory, valid for sufficiently weak scalar coupling $A\vec{I}\cdot\vec{S}$ between a set of resonant nuclear spins I and nonresonant spins S, yields the

following expressions for the rates $1/T_1$ and $1/T_2$ (Ref. 34):

$$\frac{1}{T_1} = P\frac{2}{3}\left[\frac{A}{\hbar}\right]^2 S(S+1)\frac{\tau}{1+(\omega_0-\omega_s)^2\tau^2} , \quad (19)$$

$$\frac{1}{T_2} = P\frac{1}{3}\left[\frac{A}{\hbar}\right]^2 S(S+1)\left\{\tau+\frac{\tau}{1+(\omega_0-\omega_s)^2\tau^2}\right\} , \quad (20)$$

where P is the probability that a resonant spin is coupled to a nonresonant spin, ω_0 and ω_s are the resonant and nonresonant Larmor frequencies, respectively, and τ is a correlation time for the local field. The correlation time may be *either* the duration of association of the two spins I and S or the spin fluctuation time of the spin S, whichever is shorter.

In the case of In-InI_3 mixtures, the spins I are the ^{115}In nuclei ($I=\frac{9}{2}$) and the spins S are the localized $5s$ electrons of the In^{2+} ion ($S=\frac{1}{2}$). However, because the $5s$ electron is located in the same ion as the resonant nucleus, in contrast, say, to Mn^{++} in H_2O, the very strong hyperfine field invalidates the use of the weak-coupling expressions given by Eqs. (19) and (20). A clear indication of the inadequacy of the theory is given by consideration of the frequency dependence of $1/T_2{}^*$ in InI_2: the observed rates increase strongly with frequency whereas Eq. (20) predicts that $1/T_2$ should be constant or should *decrease* with frequency depending on the value of τ. Now a hyperfine coupling A/h of more than 9 GHz has been reported for In^{2+} in a crystalline host.[35] This coupling is comparable with the Zeeman energy ($\omega_s/2\pi$) of the $5s$ electrons for the magnetic fields employed in our experiments. Consequently the electronic energy levels are strongly perturbed and this in turn affects the magnitude and frequency dependence of the nuclear relaxation rates.

We have derived a generalization of Eqs. (19) and (20) which includes the effects of a strong hyperfine interaction. The derivation is given in Appendix A. It is assumed that the local hyperfine field fluctuates sufficiently rapidly that there is no resolved hyperfine spectrum for nuclei possessing an electron spin. The rate of fluctuation is characterized by a single correlation time τ. The rates are given by Eqs. (A2) and (A16)

$$\left[\frac{1}{T_1}\right]_{VF} = \frac{PA^2}{2(2I+1)}\sum_{F',F,m} c_+^2(F',m+1)c_-^2(F,m)\frac{\tau}{1+[\omega(F,m;F',m+1)]^2\tau^2} , \quad (21)$$

$$\left[\frac{1}{T_2}\right]_{VF} = \frac{1}{2}\left[\frac{1}{T_1}\right]_{VF} + \frac{PA^2}{8(2I+1)}\sum_{F,F',m}[c_+(F',m)c_+(F,m)-c_-(F',m)c_-(F,m)]^2\frac{\tau}{1+[\omega(F,m;F',m)]^2\tau^2} , \quad (22)$$

where $c_\pm(F,m)$ are admixture coefficients for the spin-up and spin-down components of a state $|F,m\rangle$ of the combined electron-nucleus system [Eq. (A10)] and $\hbar\omega(F,m;F',m')$ is the energy difference between a state $|F,m\rangle$ and the state $|F',m'\rangle$. The sums are taken over all values $F,F'=I\pm\frac{1}{2}$ and $-F\leq m_F\leq F$. Explicit expressions for the coefficients and frequencies are given in Eqs. (A9) and (A17)–(A19). The generalized rates given in Eqs. (21) and (22) reduce to those given by Eqs. (19) and (20) in the limit $(A/\hbar)\ll\omega_s$, or where $(A/\hbar)\tau\ll 1$.

(ii) Comparison of theory and experiment: The sums in the expressions (21) and (22) for the relaxation rates were evaluated explicitly for various values of the magnetic field. Aside from the overall scaling provided by the probability P, there are two free parameters which can be adjusted to give the best fit to the magnetic field (frequency) dependence and relative magnitudes of the relaxation rates $1/T_2$ and $1/T_1$ for each composition. These parameters are the hyperfine coupling A and the correlation time τ. The results of this calculation are compared with the experimental observations for InI-1 and InI-2 in Figs. 8(a) and 8(b), respectively, and for InI_2 in Fig. 9. It can be seen that the generalized theory accounts for all the qualitative features of the data and is in quantiative agreement in most respects. The only case which is not fully satisfactory concerns the value of τ for InI_2. The strong magnetic field dependence of $1/T_2{}^*$ requires a value $\tau\gtrsim 200$ ps whereas the ratio $(1/T_2{}^*)/(1/T_1)$ at 16.0 MHz implies $\tau\simeq 150$ ps. This discrepancy might be due to some additional source of spin-lattice relaxation ($1/T_1$). However a more likely explanation is that for $\tau=150$ ps, $(A/\hbar)\tau\sim 5$. Thus we are in the range where the assumption of a single, average nuclear resonance line begins to fail. As a compromise value, adequate for the discussion in this paper, we take $\tau=200\pm 50$ ps for InI_2. For InI_3 the frequency dependence of $1/T_2{}^*$ is similar to that of InI_2 implying a comparable value of τ. However, there is a relatively large experimental error and since no measurements of $1/T_1$ could be made, a large uncertainty must be assigned to this value. The values of P, A, and τ determined for the single-phase mixtures are summarized in Table I.

(iii) Discussion: A number of interesting infer-

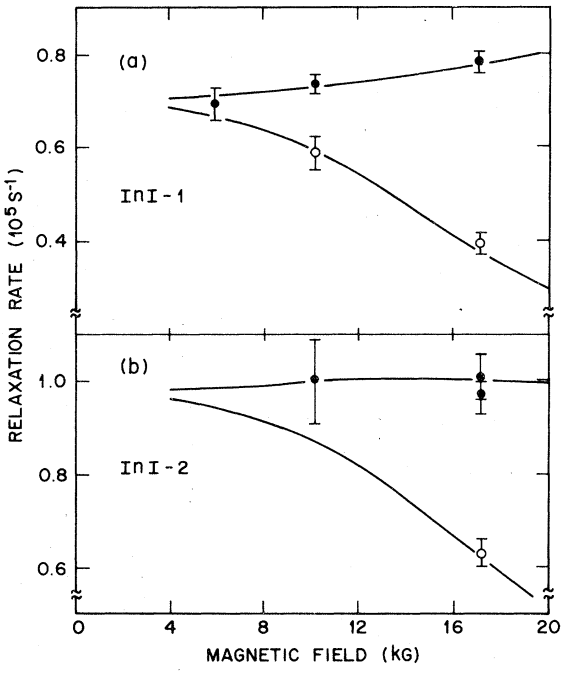

FIG. 8. Dependence of ^{115}In relaxation rates on magnetic field for two samples of nominal composition InI at 375 °C(a) and 367 °C(b). Solid points denote free-induction decay lifetimes $(1/T_2{}^*)$ and open points denote spin-lattice relaxation rates $(1/T_1)$. Solid curves show prediction of Eqs. (21) and (22) for (a) $(A/h)=8$ GHz, $\tau=14$ ps, and (b) $(A/h)=8$ GHz, $\tau=7$ ps. Theoretical curves are normalized to $1/T_2{}^*$ data points at 17.151 kG (16.0 MHz).

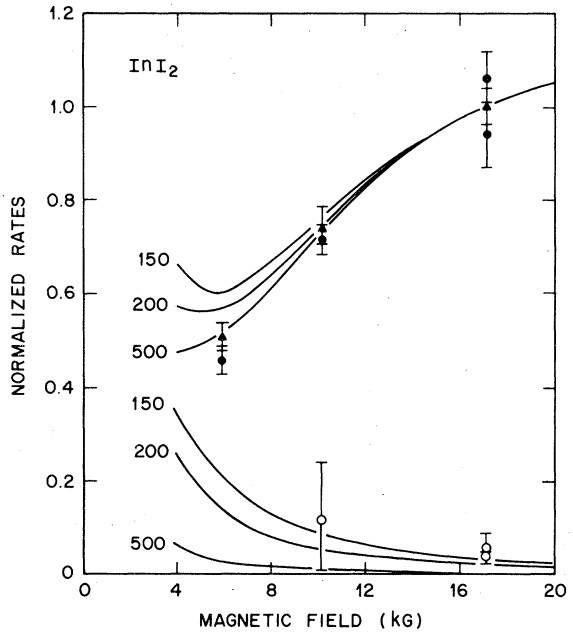

FIG. 9. Dependence of ^{115}In relaxation rates on magnetic field for liquid mixture of nominal composition InI_2 at 400 °C (triangles) and 500 °C (circles). Rates are corrected for quadrupolar background and normalized by $(1/T_2{}^*)$ values at 17.151 kG (16.0 MHz). Solid points denote normalized $1/T_2{}^*$ values and open points denote $1/T_1$ values. Curves show prediction of Eqs. (21) and (22) for $(A/h)=5$ GHz and various values of τ shown in ps. Theoretical curves are normalized to $1/T_2{}^*$ data points at 17.151 kG.

ences may be drawn from the parameters determined by the relaxation rate data. We consider first the hyperfine coupling. Values (A/h) of 8 and 5 GHz were determined independently for InI and InI_2, respectively. These may be compared with the value $(A/h)=9.362$ GHz determined by Räuber and Schneider[35] by electron-spin resonance of In^{2+} in ZnS. Since the coupling A is proportional to the probability amplitude of the $5s$ electron at the nucleus $|\psi(0)|^2$, the smaller values obtained for In-InI_3 mixtures imply wave functions which are somewhat more spread out than in the ZnS host. The larger value in InI relative to InI_2 can be understood as a consequence of the higher density of negative ions I^- in InI. These would tend to compress the In^{2+} state more in the interstitial region. InI_2, with a higher

TABLE I. Summary of parameters obtained from analysis of ^{115}In relaxation rates in liquid $In_{1-x}I_x$ mixtures: correlation time (τ), hyperfine coupling (A), activation energy for probability (ΔH), and prefactor for probability (p_0).

Sample	T(°C)	τ (ps)	A/H(GHz)	ΔH (kcal/mole)	$p_0(10^{-3})$
InI-1	375	14 ± 3	8 ± 1	6.3 ± 0.4	$1.32^{+0.47}_{-0.35}$[b]
InI-2	367	7 ± 1	8 ± 1	7.3 ± 0.7	$6.48^{+4.7}_{-2.7}$[b]
InI_2	500	200 ± 50	5.0 ± 0.5	15.4 ± 1.2	120^{+140}_{-65}[b]
InI_3	530	(200)[a]	(5)[a]	9.0 ± 1.5	(1.4)[a]

[a] p_0 for InI_3 determined by assuming values of τ and A the same as for InI_2.
[b] Error limits reflect errors in ΔH.

proportion of associated structures such as $(InI_4)^-$ presents a less confining environment.

We consider next the correlation times τ. The value of τ obtained for InI_2 is more than an order of magnitude larger than for InI. This difference is mainly responsible for the strikingly different relaxation behavior in these two compositions. An important feature of the data is that τ is essentially independent of temperature for InI and InI_2. The clearest evidence of this is provided by the data for InI where the ratio $(1/T_2^*)/(1/T_1)$ is independent of temperature. This ratio is a sensitive function of τ in both the standard and generalized theories. For InI_2, the same magnetic field dependence of $(1/T_2^*)$ is observed at 400 and 500 °C implying nearly equal τ values at these two temperatures. This feature of temperature independence together with the strong dependence on concentration suggests that τ should be interpreted as the lifetime of the In^{2+} state or, possibly, the inverse exchange frequency of the In^{2+}-In^{2+} pair. But τ is unlikely to be the spin-lattice relaxation time of the localized electron. The latter might be expected to depend strongly on temperature and to be less sensitive to composition, whereas just the opposite features are observed. Furthermore if the spin-lattice relaxation time were shorter than the lifetime or exchange time, the spins would have sufficient opportunity to polarize in the applied field and thus to produce a shift of the nuclear resonance. An estimate of this effect for InI_2 based on an assumed Curie susceptibility for the In^{2+} ions predicts an increase in (Knight) shift of roughly 0.1% over the range of the data shown in Fig. 3. Such a large paramagnetic shift is clearly incompatible with the data. Because we have not considered in detail the exchange effects and their concentration dependence, an identification of τ with the In^{2+} lifetime is only tentative; however, it can be stated with certainty that the observed values provide an upper limit on the In^{2+} lifetime and that this limit is more than an order of magnitude longer for InI_2 than for InI.

The interpretation of nuclear-relaxation data developed above implies that electronic conductivity in single-phase In-InI_3 mixtures should be viewed as a two stage process: a single-electron transfer to form a pair In^{2+}-In^{2+} from a pair In^+-In^{3+} followed by a second electron transfer after a delay of at least a time τ. Since the second transfer can proceed in either direction, there is a probability of $\frac{1}{2}$ that the complete two-stage process will result in an effective interchange

$$In^+ + In^{3+} \rightarrow In^{3+} + In^+ \ . \tag{23}$$

An interchange of this sort by a simultaneous two-electron transfer has been proposed as the conduction mechanism in Bi-BiI_3 mixtures by Raleigh.[36] The present work shows that there is an intermediate state and the data provide a measure of its lifetime.

It is easy to estimate the magnitude of the conductivity associated with the electron-transfer process and show that it is much smaller than the conductivities measured for these mixtures. We take ν_j to be the mean frequency of jumps into the In^{2+} state and can then write

$$P \simeq \nu_j \tau \ , \tag{24}$$

where we take τ to be the intermediate state lifetime. This yields, for example, $\nu_j \simeq 3 \times 10^4$ sec^{-1} for InI_2 at 500 °C. If we consider the conductivity due to an effective two-electron jump at frequency $\frac{1}{2}\nu_j$, the conductivity is approximately

$$\sigma_{\text{elec}} = \frac{c(In^+) N_0 \rho}{M} \cdot 2e \cdot \frac{1}{6} \frac{ea^2}{kT} \nu_j \ , \tag{25}$$

where N_0 is Avogadro's number, M is the molecular weight, ρ is the density, and a is the mean In-In separation ($a \sim 3$ Å). Evaluation for InI_2 at 500 °C yields

$$\sigma_{\text{elec}} \sim 4 \times 10^{-8} (\Omega \text{ cm})^{-1}$$

compared with an experimental value[7]

$$\sigma_{\text{expt}} \simeq 3.5 \times 10^{-1} (\Omega \text{ cm})^{-1} \ .$$

Similar results are obtained for InI (InI-1) for which

$$\sigma_{\text{elec}} \sim 0.8 \times 10^{-5} (\Omega \text{ cm})^{-1}$$

at 375 °C and

$$\sigma_{\text{expt}} \simeq 6 \times 10^{-1} (\Omega \text{ cm})^{-1} \ .$$

Thus in each case, the electronic conductivity is overwhelmed by the ionic contribution.

We consider next the temperature dependence of the relaxation rates. In each case the high-temperature relaxation rates can be expressed as exponential functions of temperature

$$1/T_2 \propto 1/T_1 \propto e^{-\Delta H/RT} \ . \tag{26}$$

Values of ΔH determined from semilog plots of the observed rates versus $1/T$ are given in Table I. These rates vary significantly among the different compositions reflecting, according to our model, the differing molecular structure of these mixtures. Comparison of Eq. (26) with Eq. (17) yields $\Delta H = \Delta H_3 + \frac{1}{2}\Delta H_2$. The smallest value observed for ΔH (InI-1) thus provides an upper limit on the energy required for an electron hop from In^+ to In^{3+}

$$\Delta H_2 \lesssim 14 \text{ kcal/mole} \simeq 0.6 \text{ eV} \ .$$

If InI is nearly fully dissociated, this limit would be close to the actual value of ΔH_2.

Finally, we comment briefly on the value of the preexponential p_0 of Eqs. (17) and (18). Experimen-

tal values of p_0 for each sample are given in the last column of Table I. We find that p_0 is substantially larger (more than an order of magnitude) for InI_2 than for the other compositions. This is reasonable in light of Eq. (18) since the factor $(4x-3)c_3(x)/2(2x-1)$ should be maximum near $x=0.67$, and zero for $x=0.50$ and $x=0.75$. Lacking more detailed knowledge of $c_3(x)$, a more quantitative analysis is impossible.

B. Phase-separated mixtures ($x < 0.50$)

1. *Chemical and Knight shifts*

The shift data in phase-separated liquid mixtures can be discussed separately in terms of the Knight shift in the metal-rich phase and the shift in the salt-rich phase. We consider first the metal-rich Knight shifts. The Knight shifts in all three samples having $x < 0.50$ are very close to those previously measured for pure In.[16] The temperature dependences are essentially identical to that of pure In and the magnitudes are sufficiently close that only careful differential shift measurements could determine whether the difference is real or reflects a systematic error in one or the other set of experiments. Thus within the sensitivity of these shift measurements, we find no evidence for solubility of I^- in liquid In.

The chemical shift of the salt-rich phase is indistinguishable at low temperatures from that of single-phase InI. This is consistent with the phase diagram which indicates formation of two liquid phases which are, essentially, pure In and InI. At higher temperatures, however, there is a clear tendency toward a more paramagnetic shift. This can be interpreted as due to the introduction of paramagnetic centers by the progressive solution of small amounts of In in InI as the temperature is raised.

The situation of dilute In in InI is analogous to the case of low concentrations of alkali metals in their molten halides. While it was first proposed by Rice[37] that metal enters the salt in a localized atomic state, subsequent work has favored the model proposed by Pitzer[38] in which the metal valence electron is shared by several neighboring metal ions. The description is essentially that of the F center in alkali halide crystals where an electron enters an anion vacancy and is bound to its six nearest-neighbor cations. The F-center model for metal-molten salt solutions is supported by optical studies[39,40] and a recent electron-spin-resonance investigation.[2]

If we assume that the excess electron is localized in a vacancy surrounded by z In^+ ions, the average shift experienced by the In nuclei can be expressed

$$\frac{\Delta H}{H_0}=\frac{H(\mathrm{InI})-H_0}{H_0}=\frac{zc(\mathrm{In})A_F\gamma_e}{4\gamma_n kT}\ , \tag{27}$$

where $c(\mathrm{In})$ is the mole fraction of In in the In-InI solution, γ_e and γ_n are respectively, the electronic and nuclear gyromagnetic ratios, and A_F is the hyperfine coupling of the localized electron to the neighboring In^+ ions. The shift is defined relative to the resonance position $H(\mathrm{InI})$ of stoichiometric InI, i.e., the shift observed in phase-separated mixtures near 400 °C. It is assumed that diffusion of In^+ ions relative to the paramagnetic center is sufficiently rapid compared with ω_0 that all In nuclei experience the same average shift. According to Eq. (27), the temperature dependence of the shift is due to the temperature-dependent concentration of dissolved In, $c(\mathrm{In})$, and to the explicit inverse-temperature dependence characteristic of the Curie susceptibility of the localized electrons.

The shift data alone are insufficient to determine the parameters in Eq. (27). However, it will be shown in Sec. IV B 2 that the nuclear-relaxation-rate data can be combined with the shift results to determine $zc(\mathrm{In})$ and A_F. These parameters will then be used to evaluate the validity of the F-center model.

2. *Relaxation rates*

The nuclear-relaxation data for the salt-rich phase of the two-phase mixture $In_{0.66}I_{0.34}$ are qualitatively similar to those obtained in single-phase mixtures, especially those with $x \cong 0.50$. The main differences are the much lower relaxation rates and the near equality of T_1 and $T_2{}^*$ in $In_{0.66}I_{0.34}$. In the present case we suppose the relaxation to be due to permanent paramagnetic centers associated with excess In in InI rather than to fluctuations into a paramagnetic valence state. The theoretical description of the nuclear relaxation process is nevertheless very similar in the two cases despite the different physical mechanisms involved.

The hyperfine coupling with the paramagnetic centers can be expected to be small compared with the electronic Larmor frequency ω_s. Therefore we use the standard expressions given by Eqs. (19) and (20) rather than Eqs. (21) and (22). The probability P is now to be interpreted as the probability that an In^+ ion is located next to a localized electron

$$P=zc(\mathrm{In}) \tag{28}$$

and $A=A_F$ for the F-center model. For a single electron, $S=\frac{1}{2}$ and Eqs. (19) and (20) lead to

$$\frac{1}{T_1}=\tfrac{1}{2}zc(\mathrm{In})\left(\frac{A_F}{\hbar}\right)^2\frac{\tau}{1+(\omega_0-\omega_s)^2\tau^2}\ , \tag{29}$$

$$\frac{1}{T_2}=\tfrac{1}{4}zc(\mathrm{In})\left(\frac{A_F}{\hbar}\right)^2\tau\left\{1+\frac{1}{1+(\omega_0-\omega_s)^2\tau^2}\right\}\ . \tag{30}$$

The ratio of the relaxation rates may be used to

determine the correlation time τ. We find

$$(1/T_2{}^*)/(1/T_1) = 1.14 \pm 0.05 \ ,$$

or, taking the ratio of Eqs. (29) and (30), $\tau = 1.8^{+0.3}_{-0.4}$ ps. This time is comparable with typical diffusional times in molten salts.[40] In contrast, the spin-fluctuation time obtained from electron spin resonance of Na in NaCl is of the order of 10^{-8} sec.[2] This suggests that τ should here be interpreted as the time during which a particular In^+ ion is close to the localized electron. No temperature dependence of τ can be resolved. The relatively weak temperature dependence of the ^{127}I quadrupolar relaxation indicates, in fact, that the motional correlation time is nearly independent of temperature.

Having determined the value of τ, we can use the relaxation rates and Eqs. (29) or (30) to obtain the product $zc(\mathrm{In})A_F^2$ at a particular temperature. Then since the shift yields $zc(\mathrm{In})A_F$ we can determine both $zc(\mathrm{In})$ and A_F. At 1000 °C where $\Delta H/H_0 \simeq 0.04\%$, this analysis yields

$$zc\,(\mathrm{In}) = 0.06 \pm 0.02 \ ,$$

$$(A_F/h) = 240 \pm 50 \text{ MHz} \ .$$

If we take $z = 6$, we find $c(\mathrm{In}) = 0.010 \pm 0.003$ or, equivalently, $x = 0.497$ for the composition of the InI-rich phase at 1000 °C.

The value of the hyperfine coupling obtained is solid evidence for the validity of the F-center model. For example A_F is more than an order of magnitude smaller than the hyperfine couplings obtained for the localized $5s$ electron in In^{2+}. Thus we can exclude this mechanism for the two-phase solutions. Another possibility is that In enters InI as a neutral atom. However, Hartree-Fock calculations of the core-polarization hyperfine field of the atomic $5s^25p^1$ configuration predict a value of A with magnitude roughly twice that observed and of *negative* sign.[32] As a consequence of the latter, the ("Knight") shift would become more negative as the concentration of In increases, whereas the observed variation is toward a more positive shift. Finally we compare our value of A_F, expressed as an effective magnetic field, with those determined from electron-nuclear double resonance (ENDOR) of F centers in metal halide crystals. The value of A_F given above corresponds to a local magnetic field of about 130 kG. This is intermediate between values reported for the hyperfine fields at the first-neighbor positions in the lighter alkali-metal halides, e.g., 27.3 kG for $^{23}NaCl$ and 46.7 kG for ^{39}KBr,[41] and the larger value of 305 kG reported for $^{135}BaF_2$. Since there is a general tendency for the F-center hyperfine fields to increase with increasing atomic number,[41] the intermediate value obtained for ^{115}In is therefore comparable with the crystalline F-center results.

The semilogarithmic plot in Fig. 4 shows that the relaxation rates exhibit exponential temperature dependence over a wide range. The activation energy obtained from the slope is

$$\Delta H = 10.3 \pm 0.5 \text{ kcal/mole} \ .$$

The energy ΔH can be used to estimate the critical (consolute) temperature for phase separation and the heat of solution for liquid In in InI. If we assume that the region of liquid-liquid phase separation is symmetric so that the critical point falls at a composition $In_{0.5}(InI)_{0.5}$, i.e., $x = 0.33$, the concentration of dissolved In obeys the relation[42]

$$\ln\left[\frac{2 - c\,(\mathrm{In})}{c\,(\mathrm{In})}\right] = \frac{\alpha}{RT}[1 - c\,(\mathrm{In})] \ , \tag{31}$$

where α is a parameter describing the energy of interaction of In and InI. For very low concentrations of In, $c(\mathrm{In}) \ll 1$, and Eq. (31) reduces to

$$\ln\left[\frac{2}{c\,(\mathrm{In})}\right] \simeq \frac{\alpha}{RT} \ ,$$

or

$$c\,(\mathrm{In}) \simeq 2e^{-\alpha/RT} \ . \tag{32}$$

Thus comparing with Eqs. (29) and (30), we can identify α with the activation energy ΔH determined from the measured relaxation rates. Solution of Eq. (31) at the critical point T_c yields $\alpha = 2RT_c$.[42] For $\Delta H \simeq 10$ kcal/mole, we can estimate $T_c \simeq 2500$ K. If dilute In in InI is assumed to behave like a regular solution, it can be shown[43] that $\alpha = 4\Delta h_{1/2}$, where $\Delta h_{1/2}$ is the integral heat of solution per mean mole for a mixture at the critical composition. Thus, $\Delta h_{1/2} \simeq 2.5$ kcal/mole. Alternatively, in the dilute limit the partial molar heat of solution for liquid In from pure liquid In is[43]

$$\Delta h_{\mathrm{In}} \simeq \alpha c^2(\mathrm{InI}) \simeq \alpha \ , \tag{33}$$

so that $\Delta h_{\mathrm{In}} \simeq 10$ kcal/mole.

V. SUMMARY

We have described NMR measurements of the resonance shifts and nuclear relaxation rates in a series of liquid $In_{1-x}I_x$ mixtures. The study encompassed two-phase mixtures in the range In-InI and single-phase melts InI-InI_3. The results show that the properties of these mixtures are strongly influenced by the stability of the intermediate compound InI. The mutual solubilities of In and InI were found to be very low and the critical temperature for the phase separation between In and InI is far above 1000 °C. An estimate of the consolute temperature based on the temperature dependence of the solubility of In in InI yielded $T_c \sim 2500$ K ~ 2200 °C.

The single-phase mixtures are nonmetallic and exhibit a progression of increasing chemical shifts from InI to InI_3. While InI_3 might be expected to be more covalent than InI, this trend is opposite to the trend expected from the covalency parameter in the Ramsey theory and opposite to the trend observed for molten Tl salts. This result, which we have not attempted to interpret in detail, serves to emphasize the complex origin of the chemical shift and the need to consider the variation of additional parameters such as $\langle 1/r^3 \rangle$. This is especially true when, as in the present case, more than one valence state is present.

The relaxation data in single-phase mixtures are rich in detail and yield a considerable amount of new information on the liquid structure and electron dynamics. Two distinct relaxation processes were identified. The first of these, electric quadrupolar relaxation, gives a clear indication of rotating polyatomic species for high values of x, i.e., for InI_2 and InI_3. For InI_3, the data are in rough quantitative agreement with theory for rotating dimers In_2I_6 although the analysis is not sufficiently accurate to exclude the monomer InI_3. In addition there are indications of partial dissociation at this composition. A general trend toward weaker quadrupolar relaxation was observed for both ^{115}In and ^{127}I for smaller x. This implies either (or both) a shortening of the correlation time or reduced electric field gradient on passing from InI_3 to InI. Both effects can be expected as a consequence of the replacement of covalently bonded structures In_2I_6 and $(InI_4)^-$ by a more ionic melt.

The second mechanism, specific to ^{115}In, is a relaxation process associated with fluctuations into the paramagnetic state In^{2+} by single-electron transfer. The existence of this effect demonstrates that electronic conduction is a two-step process and the nuclear-relaxation results provide an upper limit for the frequency of hopping and a lower limit for the lifetime of the intermediate state. The latter ranges from a few ps, for samples close to the composition InI, up to roughly 200 ps for InI_2. The temperature dependences of the relaxation rates depend on the hopping energy and on the concentration of In^{3+} ions. The former is estimated to be $\lesssim 0.6$ eV. The conductivity associated with this electron-transfer process is everywhere several orders of magnitude smaller than the experimentally observed conductivity. The latter is apparently dominated by ionic transport.

As a consequence of the high consolute temperature, there is very little mixing of In and InI below 1000 °C. A weak, temperature-dependent paramagnetic shift was observed for the salt-rich phase of phase-separated $In_{0.66}In_{0.34}$. This shift and a corresponding relaxation process were attributed to the effects of a low concentration of dissolved In in InI. Analysis of these data yielded a hyperfine field in good agreement with the F-center model for the dissolved metal. The concentration of the salt-rich phase at 1000 °C was determined from the same analysis to be $In_{0.503}I_{0.497}$. The activation energy of the relaxation rates (10.3 kcal/mole) is associated with the heat of solution of liquid In in InI.

ACKNOWLEDGMENT

We are indebted to G. F. Brennert for his expert technical assistance.

APPENDIX A: NUCLEAR RELAXATION VIA A STRONG SCALAR HYPERFINE INTERACTION

In this Appendix we derive a generalization of Eqs. (19) and (20) for the case of a strong scalar hyperfine interaction with a short-lived electronic spin. We consider a system of nuclear spins I and electron spins S in a magnetic field $\vec{H}_0$ with Hamiltonian

$$\mathcal{H} = -\gamma_I \hbar \vec{I} \cdot \vec{H}_0 - \gamma_s \hbar \vec{S} \cdot \vec{H}_0 + A(t) \vec{I} \cdot \vec{S} + \mathcal{H}'(t) \ , \tag{A1}$$

where the first and second terms describe the nuclear and electronic Zeeman interactions, respectively, the third term is the scalar hyperfine coupling between nucleus and electron, and the final term $\mathcal{H}'(t)$ represents the time-dependent coupling of the electronic spin to its environment. The hyperfine interaction is assumed to fluctuate randomly between two values A and 0 according to whether or not the spin is present on the nucleus of interest.

We consider here only the case in which the rate of fluctuation of the local hyperfine field is comparable with or is greater than the hyperfine coupling frequency $A/\hbar$. The full hyperfine spectrum of nuclei on atoms with an electronic spin ($A \neq 0$) and the unshifted line of nuclei with no hyperfine field ($A = 0$) then average to give a single nuclear resonance line. For the purpose of the present paper we can further assume that the probability of $A \neq 0$ is sufficiently small that the shift of the averaged resonance is negligible compared with the hyperfine coupling frequency. The relaxation rates are then given by standard theory[29] in terms of spin-correlation functions evaluated at the nuclear Larmor frequency ω_0 and at zero frequency

$$\frac{1}{T_1} = 2J^1(\omega_0) \ , \tag{A2a}$$

$$\frac{1}{T_2} = J^1(\omega_0) + \tfrac{1}{2} J^0(0) \ , \tag{A2b}$$

where the spectral density functions are

$$J^m(\omega) = \hbar^{-2} \int_{-\infty}^{\infty} dt \, e^{-i\omega t} G^m(t) \ , \tag{A3}$$

and the correlation functions are

$$G^1(t) = \tfrac{1}{4} \langle A(0) S_+(0) A(t) S_-(t) \rangle_{\text{av}} \ , \tag{A4a}$$

$$G^0(t) = \langle A(0) S_z(0) A(t) S_z(t) \rangle_{\text{av}} \ . \tag{A4b}$$

We can assume that fluctuations of the hyperfine coupling $A(t)$ are independent of those of $\vec{S}(t)$. That is, the time of association of the nuclear and electronic spin is independent of the electronic-spin fluctuations $\vec{S}(t)$ due to the interaction $\mathcal{H}'(t)$. Then Eqs. (A4a) and (A4b) can be written

$$G^1(t) = \tfrac{1}{4}PA^2 e^{-1/\tau_A}\langle S_+(0)S_-(t)\rangle_{\rm av} \ , \qquad \text{(A5a)}$$

$$G^0(t) = PA^2 e^{-1/\tau_A}\langle S_z(0)S_z(t)\rangle_{\rm av} \ , \qquad \text{(A5b)}$$

where we have introduced a correlation time τ_A which is the mean time during which $A(t)$ is nonzero and P is the instantaneous probability of nonzero A.

The spin-correlation times of Eqs. (A5a) and (A5b) can be written

$$\langle S_i(0)S_j(t)\rangle_{\rm av} = \frac{1}{N}\sum_{\alpha,\beta}\langle\langle\alpha|S_i|\beta\rangle\langle\beta|S_j(t)|\alpha\rangle\rangle_{\rm av} \ , \qquad \text{(A6)}$$

where $|\alpha\rangle$ and $|\beta\rangle$ are eigenstates of the time-independent Hamiltonian

$$\mathcal{H}_0 = -\gamma_I\hbar\vec{I}\cdot\vec{H}_0 - \gamma_s\hbar\vec{S}\cdot\vec{H}_0 + A\vec{I}\cdot\vec{S} \qquad \text{(A7)}$$

and N is the number of such eigenstates. The angular brackets $\langle\ \rangle_{\rm av}$ denote an ensemble average. The present treatment differs from the usual weak-interaction theory in that the effects of the term $A\vec{I}\cdot\vec{S}$ are included in the calculation of the spin-correlation function. This procedure accounts for the fact that the electronic energy levels are strongly perturbed by the hyperfine interactions even though, for $P \ll 1$, the average shift of the nuclear levels is small.

It is convenient to introduce the definitions

$$\tilde{S}_j(t) = e^{i\mathcal{H}'t/\hbar}S_j e^{-i\mathcal{H}'t/\hbar} \ , \qquad \text{(A8)}$$

and

$$\hbar\omega(\beta;\alpha) = E_\beta - E_\alpha \ , \qquad \text{(A9)}$$

where E_β and E_α are the eigenvalues associated with $|\beta\rangle$ and $|\alpha\rangle$, respectively. Then Eq. (A6) can be written

$$\langle S_i(0)S_j(t)\rangle_{\rm av} = \frac{1}{N}\sum_{\alpha,\beta} e^{i\omega(\beta;\alpha)t}\langle\langle\alpha|S_i|\beta\rangle\langle\beta|\tilde{S}_j(t)|\alpha\rangle\rangle_{\rm av} \ . \qquad \text{(A10)}$$

In describing the combined nucleus-electron system we choose the representation denoted by the quantum numbers F and m_F of the coupled spins. For $S = \frac{1}{2}$, the only case we consider, a state $|F,m_F\rangle$ is formed by a linear combination of two states $|m_I m_s\rangle$

$$|F,m_F\rangle = c_+(F,m_F)\,|m_F - \tfrac{1}{2},+\rangle + c_-(F,m_F)\,|m_F + \tfrac{1}{2},-\rangle \ . \qquad \text{(A11)}$$

Then substitution of Eq. (A11) into Eqs. (A10) and (A5) yields

$$G^{(1)}(t) = \frac{PA^2e^{-t/\tau_A}}{8(2I+1)}\sum_{F,F',m} e^{i\omega(F,m;F',m+1)t}c_+^2(F',m+1)c_-^2(F,m)\langle\langle+|S_+|-\rangle\langle-|\tilde{S}_-(t)|+\rangle\rangle_{\rm av} \qquad \text{(A12a)}$$

and

$$\begin{aligned} G^{(0)}(t) = \frac{PA^2e^{-t/\tau_A}}{2(2I+1)}\sum_{F,F',m} e^{i\omega(F,m;F',m)t}\big[&c_+^2(F',m)c_+^2(F,m)\langle\langle+|S_z|+\rangle\langle+|\tilde{S}_z(t)|+\rangle\rangle_{\rm av} \\ &+ c_-^2(F',m)c_-^2(F,m)\langle\langle-|S_z|-\rangle\langle-|\tilde{S}_z(t)|-\rangle\rangle_{\rm av} \\ &+ c_+(F',m)c_+(F,m)c_-(F',m)c_-(F,m) \\ &\times\langle\{\langle-|S_z|-\rangle\langle+|\tilde{S}_z(t)|+\rangle + \langle+|S_z|+\rangle\langle-|\tilde{S}_z(t)|-\rangle\}\rangle_{\rm av}\big] \ , \end{aligned} \qquad \text{(A12b)}$$

where the sums are taken over the values

$$F,F' = I \pm \tfrac{1}{2} \ \text{ and } \ -F \leq m_F \leq F \ .$$

Now we assume that the correlation functions for the spin components can be expressed in terms of simple correlation times τ_1 and τ_2

$$\langle\langle+|S_+|-\rangle\langle-|\tilde{S}_-(t)|+\rangle\rangle_{\rm av} = \langle+|S_+|-\rangle\langle-|S_-|+\rangle e^{-t/\tau_2} \ , \qquad \text{(A13)}$$

$$\langle\langle i|S_z|i\rangle\langle j|\tilde{S}_z(t)|j\rangle\rangle_{\rm av} = \langle i|S_z|i\rangle\langle j|S_z|j\rangle e^{-t/\tau_1} \ . \qquad \text{(A14)}$$

Then the final expressions for the spectral density functions are obtained by substitution of Eqs. (A13) and (A14) in Eqs. (A12a) and (A12b) and carrying out the Fourier transformation of Eq. (A3). If we define

$$\frac{1}{\tau_{1'}} = \frac{1}{\tau_1} + \frac{1}{\tau_A} \ , \qquad \text{(A15a)}$$

$$\frac{1}{\tau_{2'}} = \frac{1}{\tau_2} + \frac{1}{\tau_A} \ , \qquad \text{(A15b)}$$

the spectral functions become

$$J^1(\omega)=\frac{PA^2}{4(2I+1)}\sum_{F,F',m}c_+^2(F',m+1)c_-^2(F,m)\frac{\tau_2'}{1+[\omega(F,m;F',m+1)-\omega]^2(\tau_2')^2}\ , \tag{A16a}$$

$$J^0(\omega)=\frac{PA^2}{4(2I+1)}\sum_{F,F',m}[c_+(F',m)c_+(F,m)-c_-(F',m)c_-(F,m)]^2\frac{\tau_1'}{1+[\omega(F,m;F',m)-\omega]^2(\tau_1')^2}\ . \tag{A16b}$$

Two limiting cases of Eqs. (A15a) and (A15b) have been called scalar relaxation of the "first" and "second" kinds, respectively.[44] In the first case, $\tau_A \ll \tau_1, \tau_2$ and $\tau_{1'}=\tau_{2'}=\tau_A$. In this case the relaxation is governed by the time of association of the nuclear and electronic spins. The other limit, relaxation of the "second kind," applies when $\tau_A \gg \tau_1, \tau_2$ so that the nucleus "sees" fluctuations of the spin S.

The sums in Eqs. (A16a) and (A16b) can be evaluated for specific values of τ_1' and τ_2' once one has determined the coefficients $c_\pm(F,m)$ and the frequencies $\omega(F,m;F',m')$. These are obtained from solution of the secular equation for the Hamiltonian $\mathcal{H}_0$ given by Eq. (A7). The energies $E_{F,m}$ are[45]

$$E_{F,m}=-\frac{A}{4}-m\hbar\omega_0\pm\frac{A(2I+1)}{4}\left[1+\frac{4mx}{2I+1}+x^2\right]^{1/2}\ , \tag{A17}$$

where

$$x=\frac{2(\hbar\omega_s-\hbar\omega_0)}{A(2I+1)}$$

and the plus and minus signs are to be taken for $F=I+\frac{1}{2}$ and $F=I-\frac{1}{2}$, respectively. The energies depend on the magnetic field through the nuclear and electronic Larmor frequencies, ω_0 and ω_s, respectively. The frequencies $\omega(F,m;F',m)$ are readily calculated from Eq. (A17) by means of Eq. (A9). Finally, the coefficients $c_\pm(F,m)$ may be expressed

$$c_+(F,m)=\frac{1}{[1+r^2(F,m)]^{1/2}}\ , \tag{A18a}$$

$$c_-(F,m)=\frac{r(F,m)}{[1+r^2(F,m)]^{1/2}}\ , \tag{A18b}$$

where

$$r(F,m)\equiv\frac{c_-(F,m)}{c_+(F,m)}=\frac{E_{F,m}-\frac{1}{2}\hbar\omega_s+(m-\frac{1}{2})\hbar\omega_0-\frac{1}{2}(m-\frac{1}{2})A}{\frac{1}{2}A[(I+m+\frac{1}{2})(I-m+\frac{1}{2})]^{1/2}}\ . \tag{A19}$$

[1]For an excellent review of work on molten metal-salt mixtures see M. A. Bredig, in *Molten Salt Chemistry,* edited by M. Blander (Wiley-Interscience, New York, 1964), p. 367.

[2]M. Sosis and N. H. Nachtrieb (unpublished).

[3]R. Dupree and W. W. Warren, Jr., in *Liquid Metals 1976,* edited by R. Evans and D. A. Greenwood, IOP Conf. Proc. No. 30 (IPPS, London, 1977), p. 454.

[4]E. A. Peretti, J. Am. Chem. Soc. 78, 5745 (1956).

[5]K. Ichikawa and S. Ikawa, J. Phys. Chem. Solids 40, 249 (1979).

[6]K. Ichikawa, Can. J. Chem. 55, 2190 (1977); J. Chem. Soc., Faraday I (to be published).

[7]K. Ichikawa (unpublished).

[8]W. Klemm, Z. Anorg. Allg. Chem. 152, 252 (1926).

[9]W. Klemm and F. Dierks, Z. Anorg. Allg. Chem. 219, 42 (1934).

[10]K. H. Grothe, L. Franke, and C. Schoneborn, Naturwissenschaften 60, 473 (1973).

[11]R. E. Wood and H. L. Ritter, J. Am. Chem. Soc. 74, 1760 (1952).

[12]J. R. Beattie, T. Gilson, and G. A. Ozin, J. Chem. Soc. A, 813 (1968).

[13]E. F. Riebling and C. E. Erickson, J. Phys. Chem. 67, 307 (1963).

[14]W. G. Clark and A. L. Kerlin, Rev. Sci. Instr. 38, 1543 (1967).

[15]W. G. Clark, Rev. Sci. Instr. 35, 316 (1964).

[16]W. W. Warren, Jr. and W. G. Clark, Phys. Rev. 177, 600 (1969).

[17]S. Hafner and N. H. Nachtrieb, J. Chem. Phys. 40, 2891 (1964); 42, 631 (1965).

[18]N. F. Ramsey, Phys. Rev. 78, 699 (1950).

[19]A. F. Wells, *Structural Inorganic Chemistry* (Clarendon, Oxford, 1975), p. 356.

[20]H. Lütgemeier, Z. Naturforsch. A 19, 1297 (1964).

[21]A. Abragam, *The Principles of Nuclear Magnetism* (Oxford, London, 1961), p. 313.

[22]D. Harold-Smith, J. Chem. Phys. 59, 4771 (1973).

[23]W. W. Warren, Jr., Phys. Rev. B 3, 3708 (1971); J. Non-Cryst. Solids 8-10, 241 (1972); in *Liquid Metals 1976,* edited by R. Evans and D. A. Greenwood, IOP Conf. Proc. No. 30 (IPPS, London, 1977), p. 436.

[24]M. v. Hartrott *et al.*, in *Liquid Metals 1976,* edited by R. Evans and D. A. Greenwood, IOP Conf. Proc. No. 30 (IPPS, London, 1977), p. 460.

[25]J. Höhne *et al.*, in *Proceedings of the 7th International Conference on Amorphous and Liquid Semiconductors,* edited by W. Spear (University of Edinburgh, Edinburgh, 1977), p. 848.

[26]See, for example, A. Abragam, Ref. 21, p. 346.
[27]H. R. Brooker and T. A. Scott, J. Chem. Phys. 41, 475 (1964).
[28]G. W. Ludwig, J. Chem. Phys. 25, 159 (1956).
[29]A. Abragam, Ref. 21, Chap. VIII.
[30]R. J. C. Brown, H. S. Gutowsky, and K. Shimomura, J. Chem. Phys. 38, 76 (1963).
[31]A. Abragam, Ref. 21, p. 331.
[32]L. H. Bennett, R. F. Watson, and G. C. Carter, in *Electronic Density of States,* edited by L. H. Bennett, Natl. Bur. Stand. Spec. Publ. No. 323 (U. S. GPO, Washington, D. C., 1971), p. 601.
[33]N. Bloembergen, J. Chem. Phys. 27, 572 (1957).
[34]A. Abragam, Ref. 21, p. 311.
[35]A. Räuber and J. Schneider, Phys. Status Solidi 18, 125 (1966).
[36]D. O. Raleigh, J. Chem. Phys. 38, 1677 (1963).
[37]S. A. Rice, Discuss. Faraday Soc. 32, 181 (1961).
[38]K. S. Pitzer, J. Am. Chem. Soc. 84, 2025 (1962).
[39]E. Mollwo, Nachr. Ges. Wiss. Goett., Math-Phys., K1, 1, 203 (1935).
[40]A. Klemm, in *Molten Salt Chemistry,* edited by M. Blander (Wiley-Interscience, New York, 1964), p. 535.
[41]W. C. Holton and H. Blum, Phys. Rev. 125, 89 (1962).
[42]J. G. Kirkwood and I. Oppenheim, *Chemical Thermodynamics* (McGraw-Hill, New York, 1961), p. 137.
[43]J. G. Kirkwood and I. Oppenheim, Ref. 42, p. 176.
[44]A. Abragam, Ref 21, p. 308.
[45]N. F. Ramsey, *Molecular Beams* (Clarendon, Oxford, 1956), p. 86.